

Carrier Lifetime in ^{60}Co Gamma and 1 MeV Electron-Irradiated Tin-Doped n-Type Czochralski Silicon: Conditions for Improving Radiation Hardness

Mykola Kras'ko, Andrii Kolosiuk,* Vasyl Voitovych, and Vasyl Povarchuk

Herein, the results that determine some conditions for increasing the radiation hardness of ^{60}Co gamma or 1 MeV electron-irradiated tin-doped n-type Czochralski silicon (Cz n-Si:Sn) are presented. These conditions are determined from the analysis of the formation kinetics of dominant radiation defects (namely, VO and SnV complexes) and the recombination of charge carriers through the electronic levels of these defects in samples with different concentrations of phosphorus and tin. It is shown that low-resistivity Cz n-Si with P doping levels $>5 \times 10^{14} \text{ cm}^{-3}$ containing in addition [Sn] $\approx 10^{17}$ – 10^{19} cm^{-3} has a radiation hardening potential. In this material, the radiation degradation of carrier lifetime is several times smaller compared with Sn-free n-Si, whereas the conductivity compensation is negligible for both materials. The reduction of the lifetime degradation rate is due to a reduction of VO concentration in low-resistivity Cz n-Si:Sn.

1. Introduction

The formation of radiation-induced defects in tin-doped silicon has been the subject of intensive research for a long time. One of the first studies in this direction was reported by Brelot in 1972,^[1] but there is still interest in this topic.^[2–6] The main reason is that the isovalent tin impurity in silicon is one of the most efficient radiation-induced vacancy (V) traps. Therefore, it is suggested that Si:Sn can have a radiation hardening potential.^[7,8] Note that doping silicon with tin is a potential means of defect engineering for various nonradiation-related applications.^[9] It is also interesting that tin impurity affects the formation of nanocrystalline silicon in thin films of amorphous silicon and silicon suboxide.^[10–13]

Using the infrared absorption spectroscopy for high-dose electron-irradiated (see various studies Refs. [1,2,14]) and deep-level transient spectroscopy for low-dose electron- and proton-irradiated (see various studies Refs. [15–18]) silicon samples containing [Sn] $\approx 10^{17}$ – 10^{19} cm^{-3} , it was found that Sn acts as a selective vacancy trap and this leads to a reduced introduction


rate of the dominant electrically active vacancy-related defects in irradiated silicon: vacancy oxygen (VO or A-center), vacancy phosphorus (VP or E-center), and divacancy (V_2). However, at the same time, new electrically active SnV defects are formed, which remain stable up to ≈ 150 – 200°C .^[1,14,18] The SnV introduces two acceptor levels in the upper half of the bandgap (at $E_c - 0.21 \text{ eV}$ ($^{2-/-}$) and $E_c - 0.5 \text{ eV}$ ($^{--/0}$), E_c denotes the conduction band edge) (see other studies Refs. [16–18]) and two donor levels in the lower half of the bandgap ($E_v + 0.07 \text{ eV}$ ($^{2+/+}$) i $E_v + 0.32 \text{ eV}$ ($^{+/0}$), E_v denotes the valence band edge).^[15,16] Notably, in contrast to Sn, the isovalent lead (Pb) impurity does not create VPb-related deep levels in the upper half of the Si bandgap.^[19,20] At the same time,

the production of vacancy-related defects is quite suppressed in Pb-doped n-Si.^[2,21,22] However, a key condition for the radiation hardness of Pb-doped Si is an increase in the concentration of Pb atoms in the dispersed state and the suppression of any Pb precipitation.^[21,23]

At the same time, it becomes clear that the use of Sn doping to improve the radiation tolerance of Si parameters requires finding a balance between two processes: a reduction of V-related defects' introduction rate and the formation of SnV. A few available experimental results on the effect of Sn on the change of carrier recombination lifetime in irradiated silicon fully confirm this thesis. Earlier, it was found that the irradiation-induced lifetime degradation in Cz Si:[Sn] $= (2 - 4) \times 10^{17} \text{ cm}^{-3}$ with resistivity $\approx 2 \Omega \text{ cm}$ occurs faster in p-type Si and slower n-type Si compared with Sn-free material.^[24,25] Although in the study by Simoen et al.,^[26] it was observed that increasing the Sn concentration from 1.7×10^{18} to $6.5 \times 10^{18} \text{ cm}^{-3}$ also accelerates the carrier lifetime degradation in γ -irradiated Cz n-Si with resistivity $\approx 45 \Omega \text{ cm}$. In our previous investigation, it was found that the radiation damage of carrier lifetime in ^{60}Co γ -irradiated n-Si:Sn is determined by the phosphorus doping level, and in some cases the low-resistivity n-Si:Sn can be considered as a material with enhancement radiation tolerance.^[27,28]

We now extend our earlier studies of the recombination properties of irradiated n-Si:Sn. In this article, we will focus on defining some conditions for increasing the radiation hardness of carrier lifetime in ^{60}Co gamma or 1 MeV electron-irradiated tin-doped n-type Cz silicon. These conditions were determined using the following studies.

Dr. M. Kras'ko, Dr. A. Kolosiuk, Dr. V. Voitovych, Dr. V. Povarchuk
Laboratory of Radiation Technologies
Institute of Physics of the NAS of Ukraine
46 Nauki Ave., Kyiv 03028, Ukraine
E-mail: kolosiuk@iop.kiev.ua

 The ORCID identification number(s) for the author(s) of this article can be found under <https://doi.org/10.1002/pssa.202100209>.

DOI: 10.1002/pssa.202100209

1) We experimentally investigated the carrier lifetime degradation in ^{60}Co gamma-irradiated Cz n-Si with P doping levels between 6×10^{13} and $5 \times 10^{15} \text{ cm}^{-3}$ containing in addition $[\text{Sn}] \approx 10^{17} - 10^{19} \text{ cm}^{-3}$. Based on these data, the analysis of the formation kinetics of dominant radiation defects (namely, VO and SnV complexes) and the recombination of charge carriers through the electronic levels of these defects in samples with different concentrations of phosphorus and tin was conducted.

ii) We compared the annealing behavior of carrier lifetime in Sn-doped and control Cz n-Si after low-dose ^{60}Co gamma irradiation and subsequent isochronal annealing in the temperature range 20–440 °C.

3) The impact of Sn on the degradation of the carrier lifetime and the conductivity in low-resistivity ($\approx 2 \Omega \text{ cm}$) Cz n-Si after irradiation by 1 MeV electrons was investigated.

2. Results and Discussion

2.1. Carrier Recombination in Cz n-Si:Sn after ^{60}Co γ -Irradiation

2.1.1. Experimental Data

Figure 1 (symbols) shows the experimental dose dependences of $\Delta\tau_{\text{irr}}^{-1} = \tau^{-1} - \tau_0^{-1}$ for (a) low- and (b) high-resistivity ^{60}Co γ -irradiated Cz n-Si:Sn and control n-Si. We see that $\Delta\tau_{\text{irr}}^{-1}$ increases linearly in the investigated dose range for all samples. Accordingly, the quantitative effect of γ -irradiation on the recombination carrier lifetime in samples was estimated using the well-known relation

$$1/\tau_{\gamma} = 1/\tau_0 + k_{\tau}\Phi_{\gamma} \quad (1)$$

where τ_0 and τ_{γ} are the carrier lifetime before and after ^{60}Co γ -irradiation with a dose of Φ_{γ} and k_{τ} is the lifetime radiation damage coefficient, which is a quantitative characteristic of the sensitivity of silicon to radiation. Data fit using Equation (1) is

shown in Figure 1 by lines, and the corresponding extracted values of k_{τ} are shown in **Table 1**.

From Figure 1 and Table 1, we see that the low- and high-resistivity γ -irradiated Cz n-Si:Sn demonstrates a qualitatively different behavior of k_{τ} in comparison with Sn-free material. In the low-resistivity samples (Figure 1a), k_{τ} is smaller in n-Si:Sn compared with control n-Si and conversely in the high-resistivity samples (Figure 1b). These results are qualitatively consistent with the data of previous works.^[27,28] Also, in both cases (see Table 1), the value of k_{τ} depends on both $[\text{Sn}]$ and n_0 . In the high-resistivity n-Si:Sn with $n_0 = 7.0 \times 10^{13} \text{ cm}^{-3}$, k_{τ} increases with increasing the Sn concentration from 1.7×10^{18} (Sn2) to 6.5×10^{18} (Sn3-1) cm^{-3} . In n-Si:Sn $[\text{Sn} = 6.5 \times 10^{18} \text{ cm}^{-3}]$, k_{τ} also increases with increasing n_0 from 7.0×10^{13} (Sn3-1) to 1.0×10^{14} (Sn3-2) cm^{-3} . In the low-resistivity n-Si:Sn, k_{τ} almost does not change with increasing $[\text{Sn}]$ from 1.5×10^{17} (Sn1-1) to 3.0×10^{17} (Sn1-2) cm^{-3} and simultaneously with decreasing n_0 from 2.5×10^{15} (Sn1-1) to 1.5×10^{15} (Sn1-2) cm^{-3} .

2.1.2. Analysis of Experimental Data

The Shockley–Read–Hall (SRH) theory was used to describe the experimental data.^[29] In our experiment (n-Si, small concentration of radiation-induced defects, $\Delta n \ll n_0$, the carrier recombination occurs through a level located in the upper half of the bandgap), the carrier lifetime is determined by the lifetime of holes (minority charge carriers in n-Si), and the following expression of the SRH recombination is valid for the calculation of τ :

$$\tau_i = (\sigma_{p,i}v_p[N_i])^{-1} \left[1 + \frac{N_c \exp(-E_i/k_B T)}{n_0} \right] \quad (2)$$

where $\sigma_{p,i}$ is the cross section of hole capture by the i -th recombination center; v_p is the thermal velocity of holes; $[N_i]$ is the concentration of the i -th center with the electronic level E_i ; N_c the effective density of states in the conduction band; k_B is Boltzmann's constant; and T the absolute temperature.

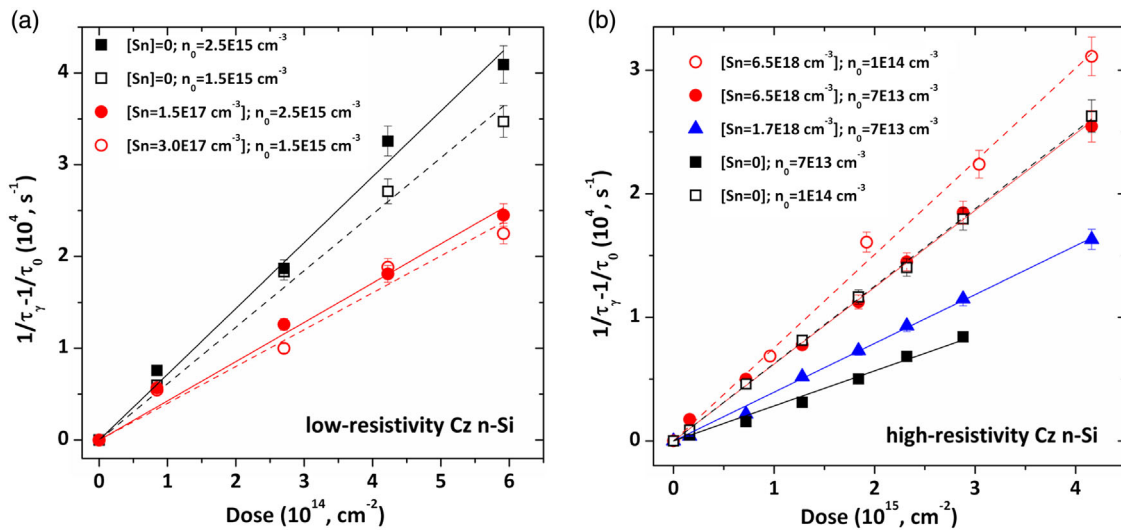


Figure 1. Dose dependences of $\Delta\tau_{\text{irr}}^{-1} = \tau^{-1} - \tau_0^{-1}$ for a) low- and b) high-resistivity ^{60}Co γ -irradiated Cz n-Si:Sn and control n-Si. Symbols: experimental data; lines: their linear approximation using Equation (1).

Table 1. Values of k_r determined from experimental data in Figure 1 using Equation (1).

Sample	Sn [cm^{-3}]	n_0 [cm^{-3}]	k_r [$\text{cm}^2 \text{s}^{-1}$]
Low-resistivity Cz n-Si			
Sn1-1	1.5×10^{17}	2.5×10^{15}	$(4.3 \pm 0.2) \times 10^{-11}$
Si1-1	0	2.5×10^{15}	$(7.2 \pm 0.2) \times 10^{-11}$
Sn1-2	3.0×10^{17}	1.5×10^{15}	$(4.0 \pm 0.2) \times 10^{-11}$
Si1-2	0	1.5×10^{15}	$(6.2 \pm 0.2) \times 10^{-11}$
High-resistivity Cz n-Si			
Sn2	1.7×10^{18}	7.0×10^{13}	$(4.0 \pm 0.1) \times 10^{-12}$
Sn3-1	6.5×10^{18}	7.0×10^{13}	$(6.2 \pm 0.1) \times 10^{-12}$
Si2	0	7.0×10^{13}	$(3.0 \pm 0.1) \times 10^{-12}$
Sn3-2	6.5×10^{18}	1.0×10^{14}	$(7.5 \pm 0.2) \times 10^{-12}$
Si3	0	1.0×10^{14}	$(6.3 \pm 0.1) \times 10^{-12}$

The VO (acceptor level of $E_c - 0.17$ eV) is the dominant recombination center at room temperature in ^{60}Co γ -irradiated Cz n-Si with P doping levels 10^{13} – 10^{17} cm^{-3} .^[30–33] Then the total change of carrier lifetime is expressed as

$$1/\tau_\gamma - 1/\tau_0 = 1/\tau_{\text{VO}} \quad (3)$$

where τ_{VO} is carrier lifetime associated with VO defect.

The main recombination centers at room temperature in ^{60}Co γ -irradiated Cz n-Si:Sn ($[\text{Sn}] \approx 10^{17}$ – 10^{19} cm^{-3}) with P doping levels 10^{13} – 10^{17} cm^{-3} are the VO and double- and single-negative acceptor levels of SnV defects.^[27,28] In this case, the total change of carrier lifetime is expressed as

$$1/\tau_\gamma - 1/\tau_0 = 1/\tau_{\text{VO}}^{\text{Sn}} + 1/\tau_{\text{SnV}(-/0)} + 1/\tau_{\text{SnV}(2-/ -)} \quad (4)$$

where $\tau_{\text{VO}}^{\text{Sn}}$, $\tau_{\text{SnV}(-/0)}$, and $\tau_{\text{SnV}(2-/ -)}$ are carrier lifetimes determined by VO in n-Si:Sn, $\text{SnV}^{(2-/ -)}$, and $\text{SnV}^{(-/0)}$, respectively.

From Equation (1), taking Equation (2)–(4) into account, we obtain expressions for the calculation of k_r .

$$k_r\{\text{VO}\} = \sigma_{\text{p,VO}} v_{\text{p}} \eta_{\text{VO}} \left(1 + \frac{N_c \exp(-E_{\text{VO}}/k_B T)}{n_0} \right)^{-1} \quad (5)$$

where $E_{\text{VO}} = E_c - 0.17$ eV; $\eta_{\text{VO}} = [\text{VO}]/\Phi_\gamma$ is the efficiency of VO formation.

$$k_r\{\text{SnV}(2-/ -)\} = \sigma_{\text{p,SnV}(2-/ -)} v_{\text{p}} \eta_{\text{SnV}} f_{2-} \left(1 + \frac{N_c \exp(-E_{\text{SnV}(2-/ -)}/k_B T)}{n_0} \right)^{-1} \quad \text{and} \quad (6)$$

$$k_r\{\text{SnV}(-/0)\} = \sigma_{\text{p,SnV}(-/0)} v_{\text{p}} \eta_{\text{SnV}} (1 - f_{2-}) \left(1 + \frac{N_c \exp(-E_{\text{SnV}(-/0)}/k_B T)}{n_0} \right)^{-1} \quad (7)$$

where $E_{\text{SnV}(2-/ -)} = E_c - 0.21$ eV, $E_{\text{SnV}(-/0)} = E_c - 0.5$ eV, and f_{2-} is the Fermi distribution function, which describes filling of the $\text{SnV}^{(2-/ -)}$ level; $\eta_{\text{SnV}} = [\text{SnV}]/\Phi_\gamma$ is the efficiency of SnV formation.

In Equation (5)–(7), the unknown parameters are σ_p and η for each recombination center. The η_{VO} and η_{Sn} values in ^{60}Co γ -irradiated Cz n-Si:Sn were obtained by analyzing the kinetics of VO and SnV formation (note that $d[\text{V}]/d\Phi = 1/J \times d[\text{V}]/dt$). In Cz n-Si:Sn irradiated at room temperature, all V formed as a result of the Frenkel pair decay create VO, SnV, and VP defects. Therefore, the kinetics of formation and annealing of V is described by the following equation.

$$\frac{d[\text{V}]}{dt} = \lambda_v - \chi_{\text{VO}}[\text{V}][\text{O}] - \chi_{\text{SnV}}[\text{V}][\text{Sn}] - \chi_{\text{VP}}[\text{V}][\text{P}] \quad (8)$$

where λ_v is the vacancy generation rate at room temperature; χ_{VO} , χ_{SnV} , and χ_{VP} are the capture constants of V by O, Sn, and P, respectively. The stationary concentration of V ($d[\text{V}]/dt = 0$) will be as follows.

$$[\text{V}]_{\text{st}} = \frac{\lambda_v}{\chi_{\text{VO}}[\text{O}] + \chi_{\text{SnV}}[\text{Sn}] + \chi_{\text{VP}}[\text{P}]} \quad (9)$$

Accordingly, for the kinetics of VO and SnV formation, we obtain

$$\frac{d[\text{VO}]}{dt} = \lambda_v \left(1 + \frac{\chi_{\text{SnV}}[\text{Sn}]}{\chi_{\text{VO}}[\text{O}]} + \frac{\chi_{\text{VP}}[\text{P}]}{\chi_{\text{VO}}[\text{O}]} \right)^{-1} \quad (10)$$

$$\frac{d[\text{SnV}]}{dt} = \lambda_v \left(1 + \frac{\chi_{\text{VO}}[\text{O}]}{\chi_{\text{SnV}}[\text{Sn}]} + \frac{\chi_{\text{VP}}[\text{P}]}{\chi_{\text{SnV}}[\text{Sn}]} \right)^{-1} \quad (11)$$

For calculations of the dependences of η_{VO} and η_{Sn} on $[\text{Sn}]$ using Equation (10) and (11), the $\eta_v \approx 4 \times 10^{-4} \text{ cm}^{-1}$ in ^{60}Co γ -irradiated Cz n-Si and the ratio $\chi_{\text{VP}}/\chi_{\text{VO}} \approx 20$ was taken from other studies.^[32,33] The ratio $\chi_{\text{SnV}}/\chi_{\text{VO}}$ was determined from our previous experiments (see the study by Kra'sko Ref. [27]): ≈ 4 for Sn1, ≈ 1 for Sn2, and ≈ 0.8 for Sn3. Note that the decrease in $\chi_{\text{VP}}/\chi_{\text{VO}}$ with increasing $[\text{Sn}]$ can indicate a nonuniform distribution of tin at high concentrations.

Figure 2 shows calculated dependences of η_{VO} and η_{Sn} on the Sn concentration in ^{60}Co γ -irradiated low-resistivity Cz n-Si:Sn. As shown in Figure 2, the increase in Sn concentration (from 3×10^{17} to $6.5 \times 10^{18} \text{ cm}^{-3}$) leads to a decrease in the efficiency of VO formation (from 1.4 to 0.5 cm^{-1}) and, accordingly, to an increase in the efficiency of SnV formation (from 2.5 to 3.5 cm^{-1}).

Figure 3 shows the experimental (symbols) and calculated (lines) dependences $k_r(n_0)$ for ^{60}Co γ -irradiated n-Si and n-Si:Sn in the range of $n_0 = 6 \times 10^{13}$ – $5 \times 10^{15} \text{ cm}^{-3}$. Curve 1 in Figure 3 corresponds to the contribution of VO in control n-Si calculated by Equation (5), in which only $\sigma_{\text{p,VO}}$ is the fitting parameter. The values of $\sigma_p \approx 2.5 \times 10^{-13} \text{ cm}^2$ for $\text{VO}^{(-/0)}$ is obtained, which is the same as in other studies Refs. [30,32,33]. Curves 2 and 3 in Figure 3 correspond to the cumulative contribution of VO and SnV in n-Si:Sn ($[\text{Sn}] = 3 \times 10^{17} \text{ cm}^{-3}$) (curve 2) and n-Si:Sn ($[\text{Sn}] = 6.5 \times 10^{18} \text{ cm}^{-3}$) (curve 3) calculated by Equation (5)–(7). In this case, the calculation and the experiment are in satisfactory agreement if $\sigma_{\text{p,SnV}}^{(2-/ -)} \approx 5 \times 10^{-15} \text{ cm}^2$ and $\sigma_{\text{p,SnV}}^{(-/0)} \approx 1 \times 10^{-15} \text{ cm}^2$, similar to the results in the study by Kra'sko.^[27]

From Figure 3, we see that low-resistivity ($n_0 > 5 \times 10^{14} \text{ cm}^{-3}$) Cz n-Si:Sn ($[\text{Sn}] \approx 10^{17}$ – 10^{19} cm^{-3}) has a radiation hardening

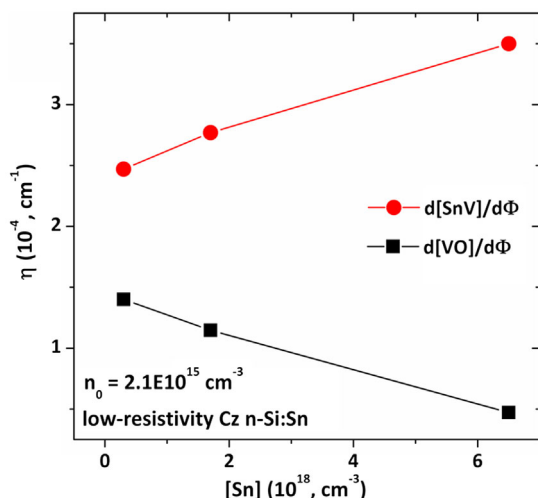


Figure 2. Calculated dependences of η_{VO} and η_{Sn} on the Sn concentration in ^{60}Co γ -irradiated Cz n-Si:Sn using Equation (10) and (11). See text for details.

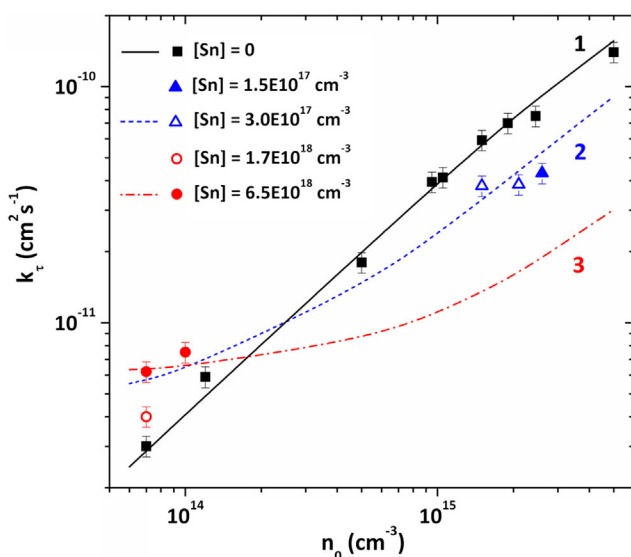


Figure 3. $k_r = (1/\tau_r - 1/\tau_0)/\Phi$ as a function of n_0 for ^{60}Co γ -irradiated Cz n-Si. Lines: calculated SRH lifetime ($\Delta n \ll n_0$); n-Si, contribution of VO; n-Si:Sn, cumulative contribution of VO and SnV.

potential. The radiation degradation of carrier lifetime occurs approximately twice as slow in Cz n-Si:[Sn $\approx 3 \times 10^{17} \text{ cm}^{-3}$] compared with Sn-free material in the range $n_0 \approx (1.5 - 3) \times 10^{15} \text{ cm}^{-3}$ (curve 1 in Figure 3). The efficiency of this process depends on the Sn concentration. Curve 3 in Figure 3 demonstrates that an increasing [Sn] to $6.5 \times 10^{18} \text{ cm}^{-3}$ causes ≈ 4.5 -fold decrease of k_r in Cz n-Si:Sn compared with the control material.

Figure 4 shows the impact of Sn concentration on k_r for (a) low- and (b) high-resistivity ^{60}Co γ -irradiated Cz n-Si:Sn. Curves in Figure 4 correspond to the cumulative (curve 1) contribution of VO (curve 2), $\text{SnV}^{(-/0)}$ (curve 3), and $\text{SnV}^{(2-/ -)}$

(curve 4) calculated by Equation (5)–(7), using the determined values of η and σ_p for VO and SnV defects.

From Figure 4, we see that k_r decreases in the low-resistivity and increases in the high-resistivity n-Si with increasing concentration of Sn. This fact can be explained by competition between the main recombination centers in Cz n-Si:Sn, namely, VO and SnV defects.

As shown in Figure 4a, the main recombination center in the low-resistivity n-Si:Sn (and in Sn-free n-Si) is VO (curve 2 in Figure 4a). In this case, tin is a competitor for oxygen in the capture of free V. The increase in Sn concentration leads to a decrease in the η_{VO} (see Figure 2) and, accordingly, k_r (curves 1 and 2 in Figure 4a). Herewith, k_r in n-Si:Sn is always smaller than in Sn-free n-Si, because both levels of SnV have smaller than VO the hole capture cross section σ_p ($\approx 1 \times 10^{-15} \text{ cm}^2$ for $\text{SnV}^{(-/0)}$, $\approx 5 \times 10^{-15} \text{ cm}^2$ for $\text{SnV}^{(2-/ -)}$, and $\approx 2.5 \times 10^{-13} \text{ cm}^2$ for $\text{VO}^{(-/0)}$).

As shown in Figure 4b, the main recombination center in the high-resistivity n-Si:Sn is $\text{SnV}^{(-/0)}$ (curve 3 in Figure 4b). Therefore, Sn can affect k_r due to a change in the η_{SnV} . Namely, the increase in Sn concentration stimulates the growth of the η_{SnV} (see Figure 2) and, as a result the increase k_r , which is shown in Figure 4b (curves 1 and 3). Comparing the absolute values of k_r for the control and Sn-doped high-resistivity n-Si (see Figure 3), we see that the lifetime degradation in n-Si:Sn is faster when $n_0 < 2 \times 10^{14} \text{ cm}^{-3}$. In this case, the large value of σ_p for VO (the main recombination center in control n-Si) is compensated by small electron filling of its level. The electron filling of $\text{SnV}^{(-/0)}$ level remains almost constant.

2.2. Carrier Recombination in Low-Resistivity Cz n-Si:Sn after ^{60}Co γ -Irradiation and Subsequent Isochronal Annealing

Figure 5 shows dependences of $(1/\tau_{\text{ann}} - 1/\tau_0)$ on the temperature of 20 min isochronal annealing in the range 20–440 °C for ^{60}Co γ -irradiated Cz n-Si and control n-Si with $n_0 = 1.5 \times 10^{15} \text{ cm}^{-3}$. The annealing behavior of carrier lifetime for both materials is similar after γ -irradiation and subsequent isochronal annealing. In the study by Kra'sko et al.,^[30] it is shown that the change of τ in ^{60}Co γ -irradiated Cz n-Si after annealing in the temperature range of ≈ 180 –350 °C is caused by the divacancy oxygen (V_2O) defect that is more recombination active than VO. In Cz n-Si:Sn, the decrease of carrier lifetime starts at ≈ 150 °C, when SnV begins to dissociate and thus increases the VO concentration.^[1,14,18] At the same time, the magnitudes of the peak changes $(1/\tau_{\text{ann}} - 1/\tau_0)$ in Cz n-Si:Sn and control n-Si are close. We also note that the carrier lifetime in Cz n-Si:Sn increases significantly after annealing above 300 °C ($\tau_{\text{ann}} \gg \tau_0$). This may indicate the gettering properties of tin.

2.3. Change in the Carrier Lifetime and the Free-Electron Concentration in Low-Resistivity Cz n-Si:Sn after 1 MeV Electron Irradiation

In Section 2.1, it was shown that the radiation degradation of carrier lifetime is several times smaller in Cz n-Si:[Sn $\approx 10^{17}$ – 10^{19} cm^{-3}] compared with Sn-free material in the range $n_0 \approx (1.5 - 3) \times 10^{15} \text{ cm}^{-3}$. At the same time, it is known that Sn

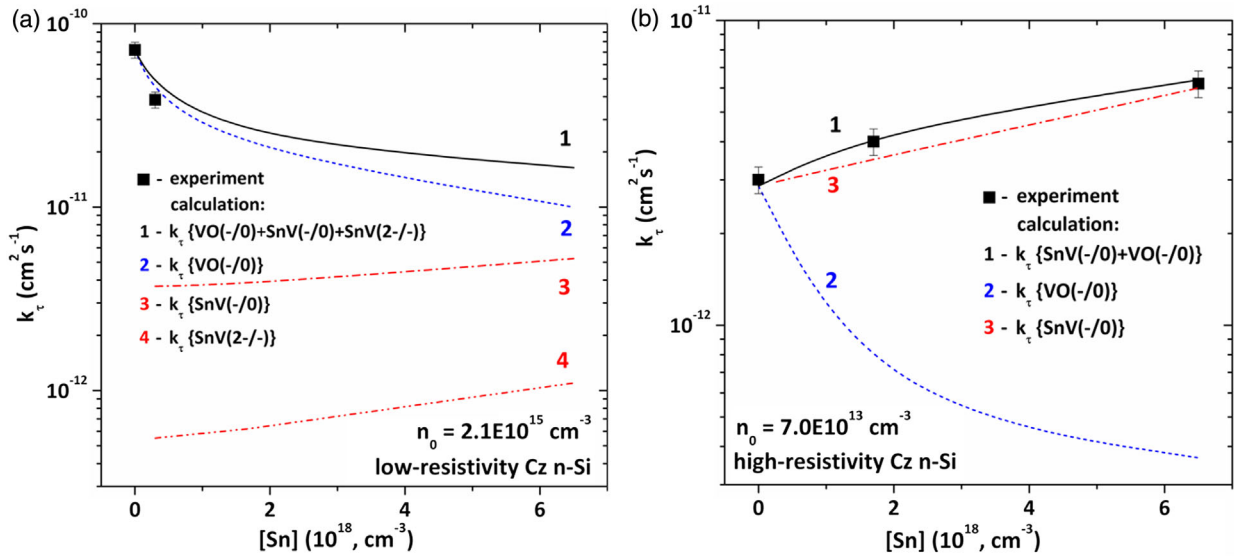


Figure 4. The impact of Sn concentration on $k\tau$ for a) low- and b) high-resistivity ^{60}Co γ -irradiated Cz n-Si:Sn. Symbols, experimental data; lines, cumulative (1) contribution of VO (curve 2), $\text{SnV}^{(-/0)}$ (curve 3), and $\text{SnV}^{(2-/^-)}$ (curve 4).

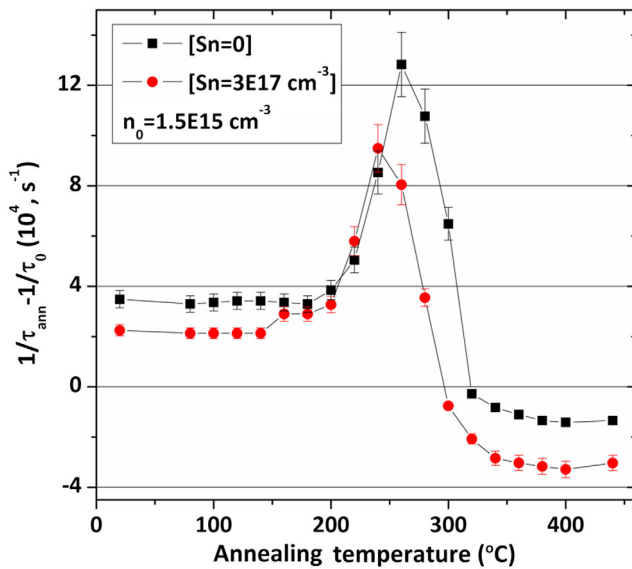


Figure 5. $1/\tau_{\text{ann}} - 1/\tau_0$ (where τ_{ann} is the carrier lifetime after each annealing step) as function of the temperature of 20 min isochronal annealing for low-resistivity Cz n-Si:Sn and control n-Si after ^{60}Co γ -irradiation with a dose of $\Phi = 5.9 \times 10^{14} \text{cm}^{-2}$.

accelerates conductivity degradation in 1 MeV electron-irradiated n-Si.^[28,34] The efficiency of these two processes will determine the radiation resistance of Cz n-Si:Sn.

Figure 6 shows the change of τ (a) and n (b) in 1 MeV electron-irradiated Cz n-Si:Sn $[\text{Sn} = 3 \times 10^{17} \text{cm}^{-3}]$ with $n_0 = 1.7 \times 10^{15} \text{cm}^{-3}$.

From Figure 6, we see that the change $(1/\tau_e - 1/\tau_0)$ is ≈ 2 times smaller in n-Si:Sn compared with Sn free n-Si, whereas the change $(n - n_0)$ is ≈ 4 times larger. In our case, the conductivity compensation becomes noticeable in n-Si:Sn after irradiation by 1 MeV electrons at room temperature to a dose of $\approx 4 \times 10^{15} \text{cm}^{-2}$ (see Figure 6b).

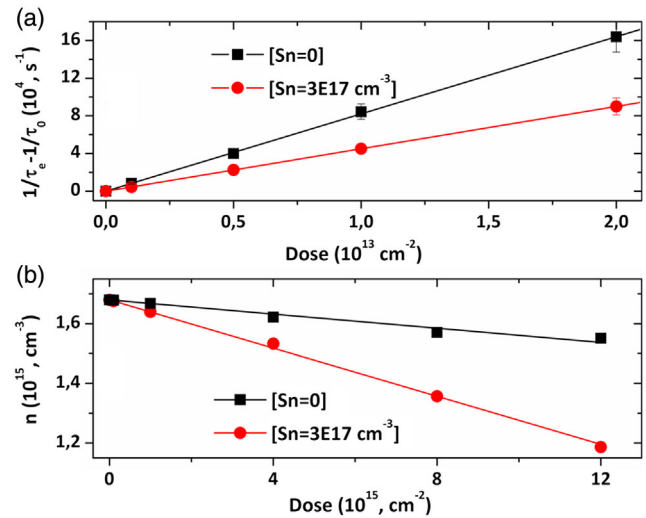


Figure 6. The impact of Sn on dose dependences of a) $1/\tau_e - 1/\tau_0$ and b) n in 1 MeV electron-irradiated Cz n-Si.

3. Conclusion

Based on the relaxation of nonequilibrium photoconductivity measurements, we investigated the carrier lifetime degradation in ^{60}Co gamma and 1 MeV electron-irradiated Cz n-Si with P doping levels between 6×10^{13} and $5 \times 10^{15} \text{cm}^{-3}$ containing in addition $[\text{Sn}] \approx 10^{17} - 10^{19} \text{cm}^{-3}$. Also, the analysis of the formation kinetics of VO and SnV defects and the recombination of charge carriers through the electronic levels of these defects in samples with different concentrations of phosphorus and tin was conducted. Moreover, the impact of Sn on the degradation of conductivity in low-resistivity Cz n-Si ($\approx 2 \Omega \text{cm}$) after irradiation by 1 MeV electrons was investigated. It is shown that the addition of $[\text{Sn}] \approx 10^{17} - 10^{19} \text{cm}^{-3}$ to low-resistivity Cz n-Si with P doping

Table 2. Sample parameters.

Sample	Sn [cm^{-3}]	n_0 [cm^{-3}]	O_i [cm^{-3}]	C_s [cm^{-3}]	τ_0 [μs]
Sn1-1	$(1.5\text{--}2.0) \times 10^{17}$	$(2.0\text{--}2.6) \times 10^{15}$	$(7.0\text{--}8.0) \times 10^{17}$	$(0.7\text{--}2.0) \times 10^{17}$	25–60
Sn1-2	$(3.0\text{--}3.5) \times 10^{17}$	$(1.5\text{--}2.1) \times 10^{15}$	$(7.0\text{--}8.0) \times 10^{17}$	$(0.7\text{--}2.0) \times 10^{17}$	30–60
Sn2	1.7×10^{18}	$(6.0\text{--}7.0) \times 10^{13}$	$(6.5\text{--}7.5) \times 10^{17}$	$< 5 \times 10^{16}$	115–130
Sn3	6.5×10^{18}	$(7.0\text{--}10) \times 10^{13}$	$(6.0\text{--}7.0) \times 10^{17}$	$< 5 \times 10^{16}$	50–75

levels $> 5 \times 10^{14} \text{ cm}^{-3}$ reduces the radiation degradation of carrier lifetime several times in comparison with Sn-free n-Si, whereas the conductivity compensation is negligible for both materials. The reduction of the lifetime degradation rate is due to a reduction of VO concentration in low-resistivity Cz n-Si:Sn. It was also found that the annealing behavior of carrier lifetime in both Cz n-Si:Sn and Sn-free n-Si is similar after low-dose ^{60}Co gamma irradiation and subsequent isochronal annealing in the temperature range 20–440 °C. At the same time, the carrier lifetime in Cz n-Si:Sn increases significantly after annealing above 300 °C ($\tau_{\text{ann}} \gg \tau_0$). We suppose this may indicate the gettering properties of tin.

4. Experimental Section

n-type Cz silicon with P doping levels between 6×10^{13} and $5 \times 10^{15} \text{ cm}^{-3}$ containing in addition [Sn] $\approx 10^{17}\text{--}10^{19} \text{ cm}^{-3}$ were used for the study. The samples were doped in the melt with Sn during the Cz crystal growth. The parameters of the investigated sample groups (the concentrations of interstitial oxygen [O_i], substitutional carbon [C_s], and tin [Sn] atoms; the initial free-electron concentration n_0 ; the initial carrier lifetime τ_0) are shown in Table 2. As control material, we used Sn-free Cz n-Si samples with similar concentrations of phosphorus, oxygen, and carbon.

The Sn concentrations were determined by secondary-ion mass spectroscopy during a series of previous studies.^[17,19,20,26] The [O_i] and [C_s] values were determined from measurements of the intensity of the absorption bands at 1107 and 607 cm^{-1} with the use of the calibration coefficients of 3.14×10^{17} and $0.94 \times 10^{17} \text{ cm}^{-2}$, respectively. The recombination carrier lifetime was derived at room temperature from the relaxation of nonequilibrium photoconductivity at low excitation ($\Delta n/n_0 \approx 1\%$, Δn is the concentration of nonequilibrium carriers). The experimental setup and lifetime measurement procedure are presented in the study by Kra'sko et al. Ref. [30]. The free-electron concentration (n) was determined using Hall effect (the details are described in another study Ref. [35]).

The samples were irradiated at room temperature with γ -rays from a ^{60}Co source ($E_\gamma \approx 1.25 \text{ MeV}$) with doses (Φ) in the range from 8.45×10^{13} to $4.16 \times 10^{15} \text{ cm}^{-2}$ (intensity of irradiation $J_\gamma \approx 2 \times 10^{11}$ photons $\text{cm}^{-2} \text{ s}^{-1}$) or 1 MeV electrons with Φ in the range from 1×10^{12} to $1.2 \times 10^{16} \text{ cm}^{-2}$ ($J_e \approx 3 \times 10^{11}$ electrons $\text{cm}^{-2} \text{ s}^{-1}$).

To study the annealing behavior of carrier lifetime in irradiated Cz n-Si:Sn, the isochronal (20 min) annealing of ^{60}Co γ -irradiated samples was conducted out in an open furnace at temperatures between 20 and 440 °C (20 °C step).

The impact of ^{60}Co γ -irradiation on the recombination carrier lifetime in samples was estimated using Equation (1). The experimental k_r values for investigated samples were determined from the linear (initial) dose dependences of $\Delta\tau_{\text{irr}}^{-1} = \tau_{\text{irr}}^{-1} - \tau_0^{-1}$.

Conflict of Interest

The authors declare no conflict of interest.

Data Availability Statement

Research data are not shared.

Keywords

carrier lifetimes, gamma and electron irradiation, isovalent impurities, radiation defects

Received: April 15, 2021

Revised: June 15, 2021

Published online:

- [1] A. Brelot, *IEEE Trans. Nucl. Sci.* **1972**, 19, 220.
- [2] C. A. Londos, D. Aliprantis, E. N. Sgourou, A. Chroneos, P. Pochet, *J. Appl. Phys.* **2012**, 111, 123508.
- [3] S.-R. G. Christopoulos, D. C. Parfitt, E. N. Sgourou, C. A. Londos, R. V. Vovk, A. Chroneos, *J. Mater. Sci.: Mater. Electron.* **2016**, 27, 4385.
- [4] E. N. Sgourou, T. Angeletos, A. Chroneos, C. A. Londos, *J. Mater. Sci.: Mater. Electron.* **2017**, 28, 10298.
- [5] I. Matyash, I. Minailova, B. Serdega, *Mater. Sci. Semicond. Process.* **2017**, 71, 263.
- [6] A. Abdurrazzaq, A. T. Raji, W. E. Meyer, *Silicon*, **2021**, 13, 1969, <https://doi.org/10.1007/s12633-020-00548-5>.
- [7] C. Claeys, E. Simoen, V. B. Neimash, A. Kraitichinskii, M. Kras'ko, O. Puzenko, A. Blondeel, P. Clauws, *J. Electrochem. Soc.* **2001**, 148, G738.
- [8] A. Chroneos, C. A. Londos, E. N. Sgourou, P. Pochet, *Appl. Phys. Lett.* **2011**, 99, 241901.
- [9] W. Lan, Y. Sun, T. Zhao, D. Yang X. Ma, *Silicon* **2020**, 12, 1433.
- [10] V. V. Voitovych, V. B. Neimash, N. N. Krasko, A. G. Kolosiyuk, V. Y. Povarchuk, R. M. Rudenko, V. A. Makara, R. V. Petrunya, V. O. Juhimchuk, V. V. Strelchuk, *Semiconductors* **2011**, 45, 1281.
- [11] V. B. Neimash, A. O. Goushcha, L. L. Fedorenko, P. Y. Shepelyavyy, V. V. Strelchuk, A. S. Nikolenko, M. V. Isaiev, A. G. Kuzmich, *J. Nanomater.* **2018**, 1243685.
- [12] R. M. Rudenko, O. O. Voitsihovska, V. V. Voitovych, M. M. Kras'ko, A. G. Kolosiyuk, V. Y. Povarchuk, M. P. Rudenko, L. M. Knorozok, *Ukr. J. Phys.* **2020**, 65, 236.
- [13] V. V. Voitovych, R. M. Rudenko, A. G. Kolosiyuk, M. M. Krasko, V. O. Juhimchuk, M. V. Voitovych, S. S. Ponomarov, A. M. Kraitichinskii, V. Y. Povarchuk, V. A. Makara, *Semiconductors* **2014**, 48, 73.
- [14] B. G. Svensson, J. Svensson, J. L. Lindström, G. Davies, J. W. Corbett, *Appl. Phys. Lett.* **1987**, 51, 2257.
- [15] G. D. Watkins, J. R. Troxell, *Phys. Rev. Lett.* **1980**, 44, 593.
- [16] J. J. Goubet, J. Sherman Christensen, P. Mejlholm, A. Nylandsted Larsen, in *Proc. 2-st ENDEASD Workshop*, (Ed.: C. Claeys), Kista-Stockholm, Sweden **2000**, 137.
- [17] E. Simoen, C. Claeys, V. B. Neimash, A. Kraitichinskii, N. Krasko, O. Puzenko, A. Blondeel, P. Clauws, *Appl. Phys. Lett.* **2000**, 76, 2838.

- [18] A. Nylandsted Larsen, J. Goubet, P. Mejlholm, J. Sherman Christensen, M. Fanciulli, H. Gunnlaugsson, G. Weyer, J. Wulff Petersen, A. Resende, M. Kaukonen, R. Jones, S. Öberg, P. Briddon, B. Svensson, J. Lindström, S. Dannefaer, *Phys. Rev. B* **2000**, 62, 453.
- [19] M.-L. David, E. Simoen, C. Claeys, V. B. Neimash, M. Kras'ko, A. Kraitchinskii, V. Voytovych, A. Kabaldin, J. F. Barbot, *Solid State Phenom.* **2005**, 108–109, 373.
- [20] M. L. David, E. Simoen, C. Clays, V. B. Neimash, M. Kras'ko, A. Kraitchinskii, V. Voytovych, A. Kabaldin, J. F. Barbot, *J. Phys.: Condens. Matter* **2005**, 17, S2255.
- [21] V. B. Neimash, V. V. Voitovych, M. M. Kras'ko, A. M. Kraitchinskii, O. M. Kabaldin, Y. V. Pavlovs'kyi, V. M. Tsmots, *Ukrayins'kij Fizichnij Zhurnal (Kiev)* **2005**, 50, 1273.
- [22] E. N. Sgourou, D. Timerkaeva, C. A. Londos, D. Aliprantis, A. Chroneos, D. Caliste, P. Pochet, *J. Appl. Phys.* **2013**, 113, 113506.
- [23] V. B. Neimash, V. V. Voitovych, A. M. Kraitchinskii, L. I. Shpinar, M. M. Kras'ko, V. M. Popov, A. P. Pokanevych, M. I. Gorodys'kyi, Y. V. Pavlovs'kyi, V. M. Tsmots, A. Kabaldin, *Ukrayins'kij Fizichnij Zhurnal (Kiev)* **2005**, 50, 492.
- [24] V. B. Neimash, M. G. Sosnin, B. M. Turovskii, V. I. Shakhovtsov, V. L. Shindich, *Sov. Phys. Semicond.* **1982**, 16, 577.
- [25] Y. M. Dobrovinskii, M. G. Sosnin, V. M. Tsmots', V. I. Shakhovtsov, V. L. Shindich, *Sov. Phys. Semicond.* **1988**, 22, 727.
- [26] E. Simoen, C. Claeys, A. Kraitchinskii, M. Kras'ko, V. B. Neimash, L. I. Shpinar, *Solid State Phenom.* **2002**, 82–84, 425.
- [27] M. M. Kras'ko, *Ukr. J. Phys.* **2012**, 57, 1162.
- [28] M. Kras'ko, A. Kraitchinskii, A. Kolosiuk, V. Voitovych, R. Rudenko, V. Povarchuk, *Solid State Phenom.* **2014**, 205–206, 323.
- [29] E. Gaubas, E. Simoen, J. Vanhellemont, *ECS J. Solid State Sci. Technol.* **2016**, 5, 3108.
- [30] M. Kras'ko, A. Kolosiuk, V. Voitovych, V. Povarchuk, *Phys. Status Solidi A* **2019**, 216, 1900290.
- [31] I. I. Kolkovskii, P. F. Lugakov, V. V. Shusha, *Phys. Status Solidi A* **1984**, 83, 299.
- [32] S. Zubrilov, S. V. Koveshnikov, *Fiz. Tekh. Poluprovodn.* **1991**, 25, 1332.
- [33] M. M. Kras'ko, V. B. Neimash, A. M. Kraitchinskii, A. G. Kolosiuk, O. M. Kabaldin, *Ukr. J. Phys.* **2008**, 53, 683.
- [34] M. M. Kras'ko, *Ukr. J. Phys.* **2013**, 58, 243.
- [35] M. M. Kras'ko, A. G. Kolosiuk, V. B. Neimash, V. Y. Povarchuk, I. S. Roguts'kyi, A. O. Goushcha, *J. Mater. Res.* **2021**, 36, 1646.